



# Burnback Analysis of 3-D Star Grain Solid Propellant

K Obula Reddy<sup>1</sup>, K M Pandey<sup>2</sup>

<sup>1</sup>PG Student, Department of Mechanical, NIT Silchar, Assam, India, obulareddy.bec10@gmail.com

<sup>2</sup>Professor, Department of Mechanical, NIT Silchar, Assam, India, kmpandey2001@yahoo.com

## Abstract

Determination of the grain geometry is an important and critical step in the design of solid propellant rocket motors, because accurate calculation of grain geometrical properties plays a vital role in performance prediction. The performance prediction of the solid rocket motor can be achieved easily if the burn back steps of the grain are known. In this study, grain burn back analysis for 3-D star grain geometries for solid rocket motor was investigated. The design process involves parametric modeling of the geometry in CAD software through dynamic variables that define the complex configuration. Initial geometry is defined in the form of a surface which defines the grain configuration. Grain burn back is achieved by making new surfaces at each web increment and calculating geometrical properties at each step. Equilibrium pressure method is used to calculate the internal ballistics. The procedure adopted can be applied to any complex geometry in a relatively simple way for preliminary designing of grain configuration.

**Key words:** 3D grains, grain burning regression, internal ballistics, solid rocket motor.

## Nomenclature

$P_c$  = chamber pressure  
 $V_c$  = gas cavity volume  
 $\rho_b, \rho_c$  = solid and gas density of propellant  
 $A_b$  = burning area of solid propellant  
 $r_b$  = burning rate  
 $A_t$  = throat area  
 $V_{int}$  = static volume occupied by ignition system  
 $A_p$  = port area  
 $l$  = length of axial grain  
 $V_f$  = total internal volume of SRM  
 $I_{anlyst}$  = Total Number of Segments  
 $c^*$  = Characteristic Exhaust Velocity  
 $C_F$  = Nozzle Thrust Coefficient  
 $y$  = Burn Distance  
 $P_e$  = nozzle exit pressure  
 $P_{amb}$  = ambient pressure  
 $\mathcal{E}$  = area ratio  
 $\gamma$  = specific heat ratio  
 $W$  = web burnt thickness  
 $n$  = no. of star vertex  
 $\theta$  = star point semi angle  
 $F$  = thrust  
 $a$  = burn rate coefficient

## 1. Introduction

In today's modern warfare, most of the weapon systems used needs some kind of propulsive system that helps them to move from one location to another location. For complex weapon systems like airplane and so on, a very complex propulsive system is required. For simple weapon systems like artillery rockets or surface to air rockets, cheaper, simpler and maintenance free propulsive systems is required. The solid rocket motors are most common used propulsive systems for these types of applications. In many military and civilian applications, solid propellant rocket motors with different types of thrust-time profiles are required according to the characteristics of the mission. If the propellant (and therefore its properties) is fixed, the main parameter affecting the thrust-time profile is the grain geometry. The change in the grain geometry during operation of the rocket motor causes the burn area to change, therefore the thrust of the motor changes. Grain burn back analysis is the determination of the change in the grain geometry during the operation of the rocket motor. The grain geometry and hence the burn area changes due to the regression of the propellant surface during burning. The pressure of the rocket motor can be calculated if the burning area is known. From the burn back analysis, very useful data can be obtained such as:

- The mass of the propellant remaining and the instantaneous mass of the rocket motor,
- The sliver fraction,
- The place and amount of expected thermal loading,
- The grain deformation or fracture, either from stress or geometric reasons,
- The port area for every burn step, therefore the erosive burning characteristic.

By the analysis of grain burn back we can get the above most important data, because from this data we can easily go through for design of rocket, because the performance parameters are greatly effect by the above obtained data that's why, we can say that the grain burn back analysis is plays an main great role play in the design of rocket and performance analysis. Grain design is to evolve burning surface area and develop it's relation with web burnt. 3D grains are complex in shape; hence their design methodology is also

complicated. Different methods have been used to calculate the geometrical properties of grain burn back analysis [1, 2]. The methodology adopted in this work is CAD modeling of the propellant grain. A parametric model with dynamic variable is created that defines the grain geometry. A surface offset is used to simulate grain burning regression, and subsequent volume at each step is evaluated.

## 2. Burn back analysis using solid modeling

### 2.1 Geometrical modeling of the propellant grain

The burn back methodology used in this study is solid modeling of the propellant grain. In general, the solid propellant grain at the beginning of the operation is

modeled parametrically. The parameters that change during the burn back process are decided and for every burn step they are modified accordingly. The grain geometry is based on CAD and PRO-E software that has the capability of handling parametric modeling. Grain is modeled in parts to provide ease and ensure lesser chances of surface creation failure. A simple variable input is sufficient to create the geometry. A detailed description of the grain modeling is follows like, first of all for modeling the initial grain some parameters have to know, those are grain length in combustion chamber case, star grain inner radius and outer radius or the web burn thickness. The following parameters listed here are useful for developing the initial star grain of the geometry.

Table1. The SRM geometrical data are given below

Section	$l$ (mm)	W (mm)	$R_1$ (mm)	$R_2$ (mm)	$R_3$ (mm)	$R_4$ (mm)	n	$\theta$ ( $^\circ$ )
A	500	27.55	15.748	63	35.94	----	6	30

The geometrical entities necessary to define the star cross section of the solid propellant grain is follows like:  $l$  the grain length of the section,  $w$  the grain web burn thickness,  $R_1$  the in word star leg radius,  $R_2$  the grain outside radius or the combustion chamber inside radius by neglecting the coating material,  $R_3$  grain outward leg radius,  $R_4$  fillet or blend radius it is applicable after some burn steps of the propellant like here in second case and the third case of solid modeling of the grain,  $\theta$  star point semi angle. Once the Grain configuration variables have been defined, following steps are taken to construct the grain. Grain boundary is a revolve protrusion in the form of a solid with no burning surface. Grain bore is a revolved surface with all surfaces burning. Boolean function is used to subtract the solid within grain bore. Similar operation is performed for fins and slots. All surfaces defined by fin and slot are burning. The solid form is parametric and can change with change in grain variables. The final solid is the required grain configuration.

### 2.2 Burn rate

Burn rate is one of two major variables of the mass flow, yet many factors affect the burn rate itself. Composition of the propellant plays a major role but is predetermined. Moreover the composition is usually the same throughout the entire propellant mass. So by experimentally determining the properties of the propellant composition we can leave

out much of its properties as they will not have an effect on variable performance. Therefore if the other affecting factors are negligible the burn rate is very predictable. The conditions affecting the burn rate are [2] [3]:

- First and foremost the pressure in the combustion chamber.
- Initial temperature of the propellant.
- Gas flow along burning surface.
- Motion of the rocket (fast spinning for example).

The research towards the effects of these conditions is not yet able to provide an analytic prediction. But the effects of each of the conditions separately have been studied, and provides empirical predictions [2] [3]. Following is a deeper examination of these conditions as a background to why none are taken into account by the model, and how they could be implemented. These are not the point of focus in this model, as they have already been modeled using other models. Our focus still lies in the geometry evolution, but it is still necessary to understand what their effect might be.

#### 2.2.1 Pressure and burn rate

Experimental testing of propellants provides burn rate's dependence on pressure. Quick examination of

such experimental measurements [2] provides the following expression [4] for the relation

$$r_b = a_0 P_c^n + b \dots\dots\dots (1)$$

Where  $r_b$  is the burn rate,  $P_c$  is the pressure,  $a_0$  and  $b$  is a function of the initial temperature of the propellant and  $n$  is known as the combustion index. This relation can be simplified though, for the case of rockets where  $b$  is usually very small [3]. The simplified result

$$r_b = a_0 P_c^n \dots\dots\dots (2)$$

This is known as the Saint-Robert's or Vieille's law. Where  $a_0$  and  $n$  are found empirically for a certain propellant. They usually apply for a certain range of pressures. A set of different values for  $a_0$  and  $n$  can provide the needed relations between burning rate and pressure throughout the combustion.

### 2.2.2 Temperature and burn rate

Temperature affects the rate at which chemical reactions take place. Therefore the initial propellant temperature affects the burning rate. It is therefore common to place the rocket in a temperature controlled space, or at least protect from the sun prior to ignition. Moreover initial temperature requirements are determined, so that if conditions exceed the conditions, launch is delayed. As a rocket in-flight is exposed to extreme temperatures, from 220K up-to 344K, it is important to see how the propellant performs in these extreme variations. A typical composite propellant experiences a variation of up-to 20% to 35% in chamber pressure  $P_c$  [2]. Moreover, for such temperature variations the thrust operation time varies with the same percentage. Non uniform temperature within the grain may have an even more disastrous effect as the pressure may not be symmetric and the thrust vector alters. The effect of grain temperature on pressure is expressed as

$$\Delta P = P_0^{\pi_k \Delta T} \dots\dots\dots (3)$$

Where  $\Delta P$  is the variation of pressure from the reference pressure  $P_0$ , at a temperature variation of  $\Delta T$  with  $\pi_k$  an experimentally measured coefficient known as the temperature sensitivity of pressure at a constant burning area (K). By determining the  $a_0$  parameter for the correct reference temperature, and giving the entire propellant that uniform temperature, we can neglect the effect of a temperature difference.

### 2.3 Grain geometry

Burn rate determines how fast a propellant burns. The amount of propellant actually available for burning at that burn rate is determined by the shape of the propellant mass, the grain geometry. The burning takes place at the surface, and the amount of surface a certain shape has is determined by its geometry. The propellant mass is distributed on the inside of the combustion chamber. The mass is usually extruded or molded in a certain shape within the cylinder. In most cases the shape forms a cavity within the propellant mass, which is connected to the nozzle. This space is where hot gases move towards the nozzle. On ignition all exposed surfaces around this space will burn. When burning, the surface recedes as solid propellant turns to gas. The receding takes place in a direction that is normal to the surface. The configuration of the grain or the shape of it defines how it behaves in time. The grain is in most cases cylindrically symmetric. In that case it is sufficient to examine a two dimensional cross section of the grain. Rocket models with variations along their length axis do exist but these require more complex calculations. While a complex configuration does not necessarily provide a performance that is not achievable in a simpler constant 2D cross section model. This study will only focus on grain geometries that can be described by a three dimensional cross section. Another symmetry often found in the grain is a rotational symmetry. This is often the case because it is important to get a rotationally symmetric exhaust out of the nozzle, or else the rocket net thrust vector will not be straight. Performance of a grain is usually measured in a thrust vs. time diagram. Alternatively when neglecting burn rate effects, burn area vs. burn depth, are used instead of the thrust/time. These diagrams can easily display if a grain is progressive or regressive, which translates to growing or diminishing thrust (in our case study see results). But these can be easily described with cylindrical grains burning in or out. More complex grain is required for more complex performances. A combination of progressive followed by regressive, or constant burn, usually require more exotic shapes, like a stars or fyncocyls. (Fig. 1) The performance of a grain the model looks at is ultimately the burning surface as a function of burn depth. In a two dimensional grain it is therefore necessary to calculate the circumference of the grain along the burning interface, as a function of burn depth. The burning interface recedes radially so burn depth translates linearly to a greater circle radius. Grain geometry evolution is a problem that is best described by an interface. The interface is the front of the propellant that is burning. As the interface

propagates the geometry changes, and the amount of burning surface changes. The way to describe a propagating interface is not so simple. The interface propagation problem at hand has similarities with other physical problems. The burning front in forest fires, paper, ocean waves and crystal

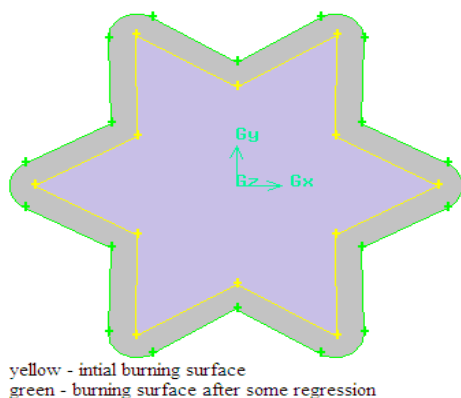


Fig.1. star propellant grain receding outward as it burns. The yellow lines show the initial and green final burn interfaces. As the interface moves outward, its length grows translating to more combustion taking place.

## 2.4 Geometrical Regression

The grain regression is achieved by a web increment equal in all direction. A web increment is selected for which the grain regression is performed. At each step new grain geometry is created automatically thereafter volume at each web increment is stored in a file. A decreasing trend is obtained for volume of the grain. The star shape is defined by parameters, where the set of chosen parameters defines a unique star shape. After producing an initial shape the star evolution is modeled, using certain reference points within the shape that do not change when evolving. As mentioned the star is made of straight sections or circle sections, and these sections are defined as functions. Polar coordinates are used and the function describing the interface is the radial distance as a function of the angle  $r(\theta)$  (Fig. 2). Points of intersection between the different sections are determined. From these points of intersection it is possible to extract the order at which certain sections burn off or disappear. Using all these points, functions and disappearance time of certain sections, it is possible to construct the shape as a function of burn depth.

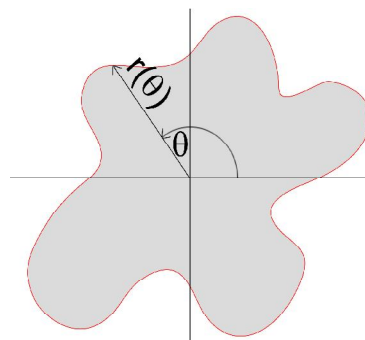


Figure 2: The radial function,  $r(\theta)$ , defined as the distance from the origin to the interface. The function  $r(\theta)$  plotted over the range  $\theta : 0 \rightarrow 2\pi$  describes the entire interface.

This method is the only method that gives an exact solution to the problem. This is due to the fact that the function describing the shape is not continuous but a piecewise-defined function. Every piece of the piecewise function is easily evolved as a function of burn depth. A straight line evolves by moving in a direction perpendicular to itself. The distance that the line is moved is equal to the burn depth. The radius will grow linearly with the burn depth (Fig. 3). Likewise a convex circle section diminishes (Fig. 4). Its radius shrinks linearly with burn depth, until the burn depth is equal to its initial radius. In that case the circle's radius has reached zero. A circle section with radius zero translates to a sharp corner. In that case the circle section is omitted altogether from further steps of calculation and the bordering function pieces intersect each other. Using all different intersection points and function pieces the ranges of every piece of the piecewise function is determined. Using the function describing the shape information is gathered: the shape is plotted, the circumference of the shape is calculated and so is the remaining area/volume of propellant and port area.

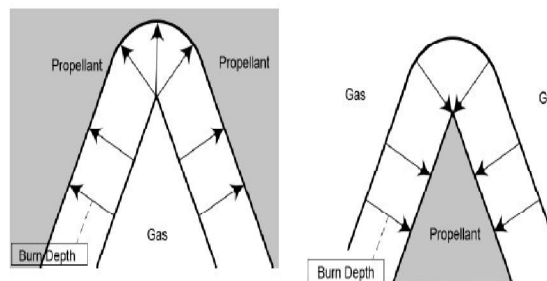


Figure: 3 & 4

Figure 3: Interface evolution of a concave shape, a sharp cusp disappears.

Figure 4: Interface evolution of a convex shape, forming a sharp cusp.

**Volume Calculation formula**

The three-dimensional gas cavity volume evolves as a function of the burning distance. This evolution can be expressed as

$$V_c(y) = \sum_{i=1}^{I_{anlyst}} A_{p_i}(y)l_i(y) - V_{int} \dots\dots\dots (4)$$

Where  $V_{int}$  is the static volume occupied by the ignition system and submerged nozzle assembly. Further, the number of segments  $I_{anlyst}$  is also noted to generally decrease during the computation process due to axially burnt out segments.

The unburnt propellant mass can then be calculated from

$$m_b^{unburnt}(y) = \rho_b (V_f - V_c(y)) \dots\dots\dots (5)$$

Where  $V_f$  is the total internal volume of the SRM. In the current implementation, it can be noted that the dome structures are taken into consideration during calculation of  $V_f$  as it gives more accurate results.

Lastly, the burnt propellant mass is determined through

$$m_b^{unburnt}(y) = \rho_b (V(y) - V(0)) \dots\dots\dots (6)$$

**3. Performance Prediction**

The motor performance is calculated using a simplified ballistic model. The pressure-time curves (pressure history) are characterized by a rapid change of pressure during the short period at *start-up* after ignition and final *tail-off* when the solid grain has been burnt. In-between, the pressure curve is dominated by a quasi-steady phase where its characteristics are determined primarily by grain geometry and its combustion. The Governing equations for the chamber pressure are derived from mass conversation, ideal gas formulations and the definition of ideal characteristic velocity. One important equation describes the change of pressure with time and takes form of a first order differential equation

$$\frac{dP_c}{dt} = \frac{RT_c}{V_c} \left[ A_b r_b \rho_b - \rho_c \frac{dV_c}{dt} - \frac{A_t P_c}{c^*} \right] \dots\dots\dots (7)$$

Where  $V_c$  is the instantaneous gas cavity volume that expands with time,  $A_b$  is the exposed propellant burning area;  $\rho_b$  and  $\rho_c$  are the solid and gas density of the propellant;  $R$  is the specific gas constant and  $T_c$  is the chamber temperature, which is independent of pressure and often assumed to be constant [5],[8]. Further, as the propellant gas density is considerably less than its solid counterpart, i.e.  $\rho_c \ll \rho_b$ . The gas density term is often neglected. With (2.7), it is thus possible to determine the complete pressure-time curve.

With known chamber pressure, the thrust for the SRM can be calculated through the following simple relation

$$F = C_F P_c A_t$$

$$C_F = \sqrt{\frac{2\gamma^2}{\gamma-1} \left(\frac{2}{\gamma+1}\right)^{\gamma+1/\gamma-1} \left[ 1 - \left(\frac{P_e}{P_c}\right)^{\gamma-1/\gamma} \right] + \frac{P_e - P_{amb}}{P_c} \epsilon} \dots\dots\dots (8)$$

If the mass of generated is equal to the mass of ejected through the nozzle then the pressure gas vicinity chamber is calculated by generating the mass balance and final the equation of steady state operation is as defined below

$$P_c = \left( \frac{\rho_p a c^* A_b}{A_t} \right)^{1/(1-n)} \dots\dots\dots (9)$$

**3.1. Volume and Area Calculations from geometrical grain data**

CAD programs can only calculate the whole surface area of a solid, whereas, the actual burning area is only at exposed uninhibited surfaces. When mandrel inflates through the full grain, the burning area is at the surface of mandrel. Let the surface area of full grain is  $A_f$  which is determined only once at the start of program. As the mandrel inflates, its surface area  $A_m$  is calculated at each burn step. After subtracting mandrel from full grain, we get grain model, whose surface area is calculated as  $A_g$ . These different areas are shown as below.

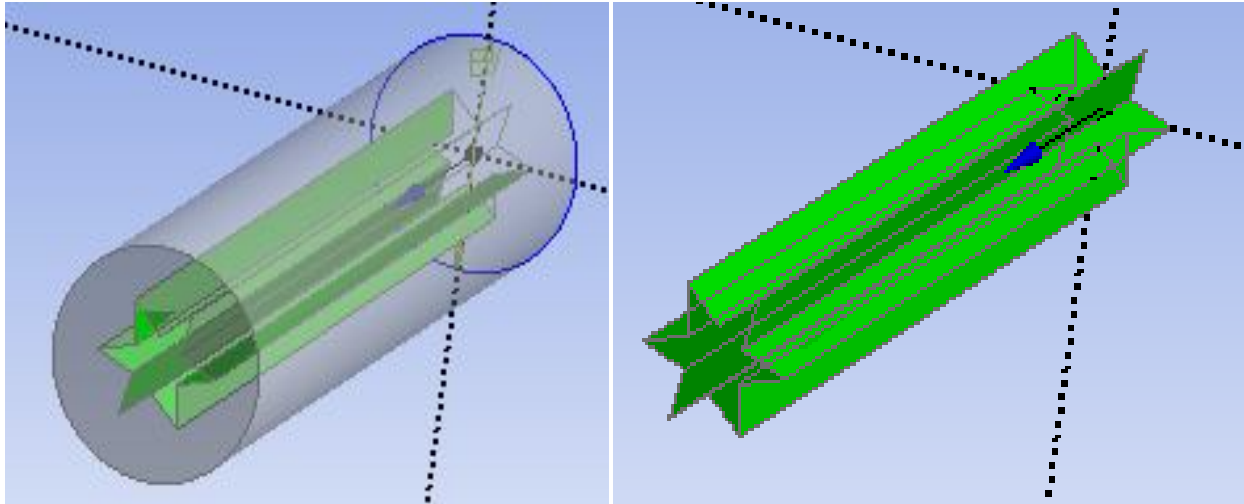


Figure 5: Grain and mandrel surface regression (0%)

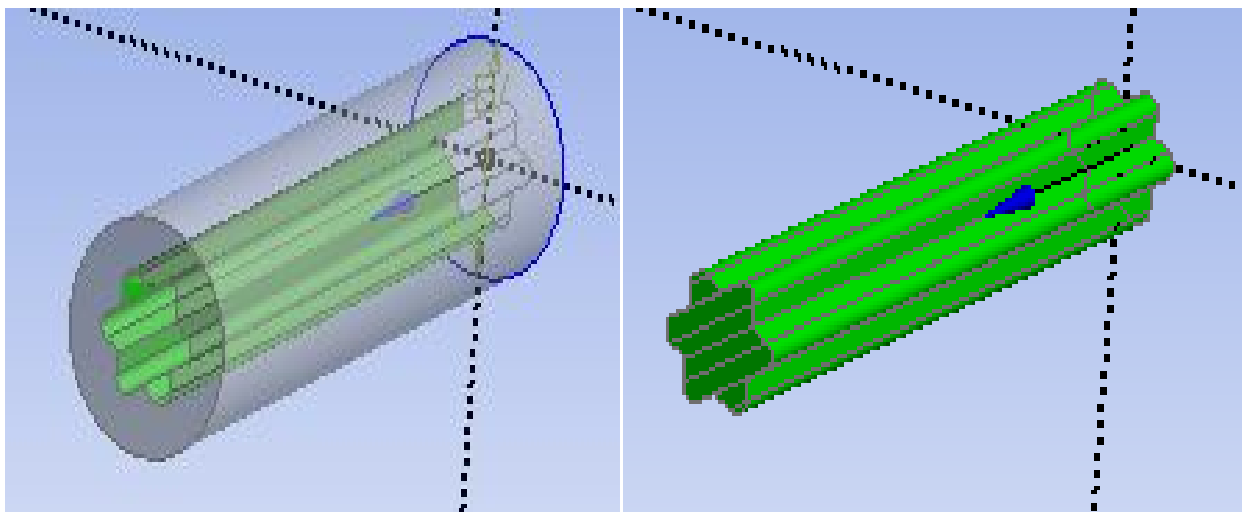


Figure 6: Grain and mandrel surface regression (30%)

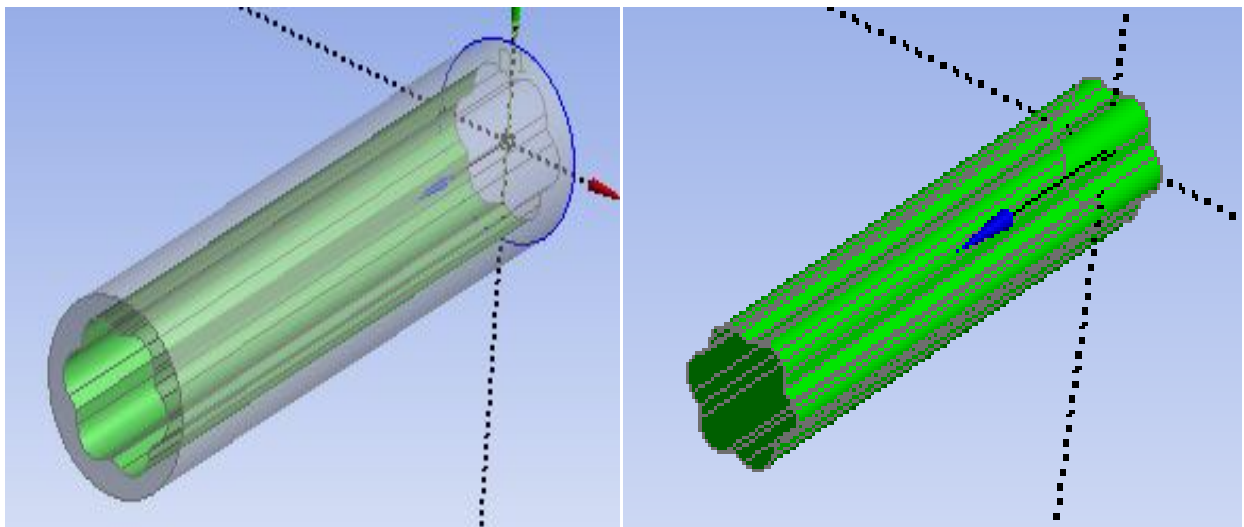


Figure 7: Grain and mandrel surface regression (70%)

#### 4. RESULTS AND DISCUSSION

The above figures shows the grain and mandrel surface regression during the combustion of solid propellant and here we are considered the three cases during the combustion and expressed in terms percentages of surface regression of both the mandrel and the grain. From these diagrams that means from this information we can predict the performance of rocket motor as explained above and we can draw the our results as various contours parameters like pressure, thrust, unburnt propellant, burnt propellant, surface area of burning and the volume of core developed and these results are drawn below as graphs. These graphs are drawn during the major operation of solid rocket motor

that's why the graphs are not mentioned fully, but these graphs defines the basic information of the star grain operation in our assumption case. From our results we can compare the results of analytical and geometrical obtained from these methods. If see some cylindrical grain structures, the type of burning is progressive and the pressure and thrust are continuously increase as the web burnt length increases, but in star grain there is a chance of obtaining three types of burning by varying the geometrical parameters during combustion. That's why now a days there is a great role of star grain solid propellant in solid rocket motor. And there is a great research is going on star grain to minimize the stress effects during combustion.

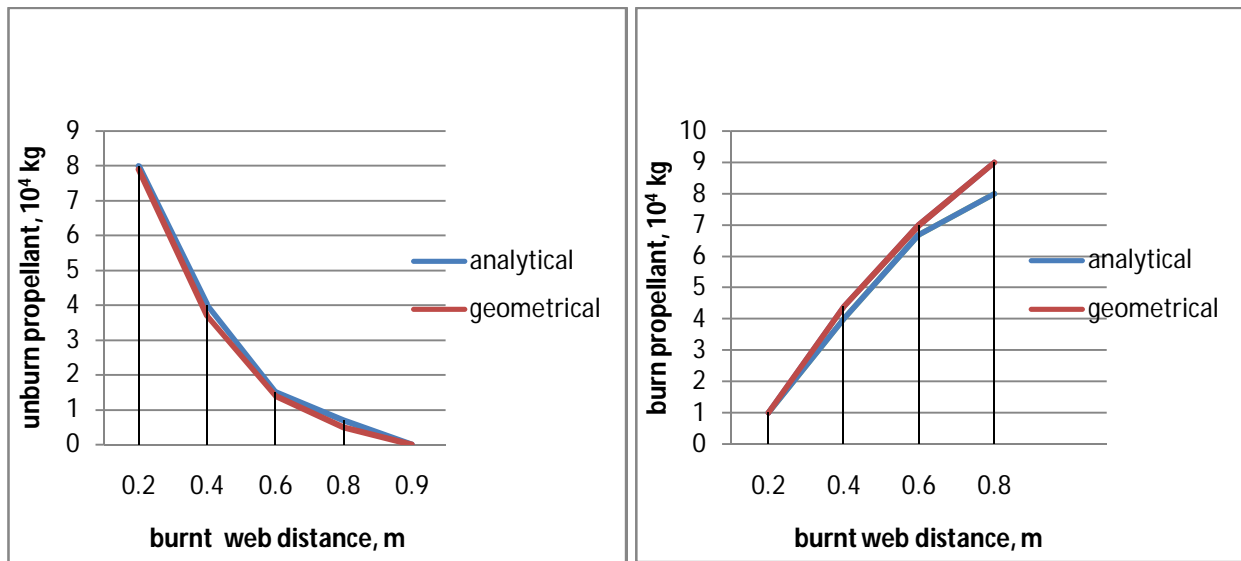


Figure 8: the graphs of web burnt – unburnt/burnt propellants

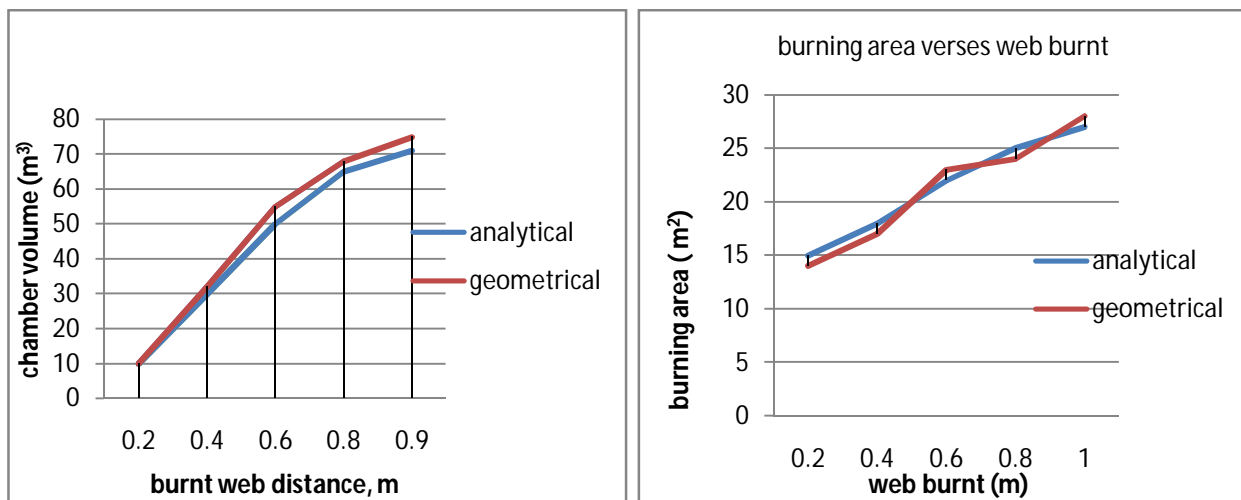


Figure 9: the graphs of burnt web – chamber volume/burning area



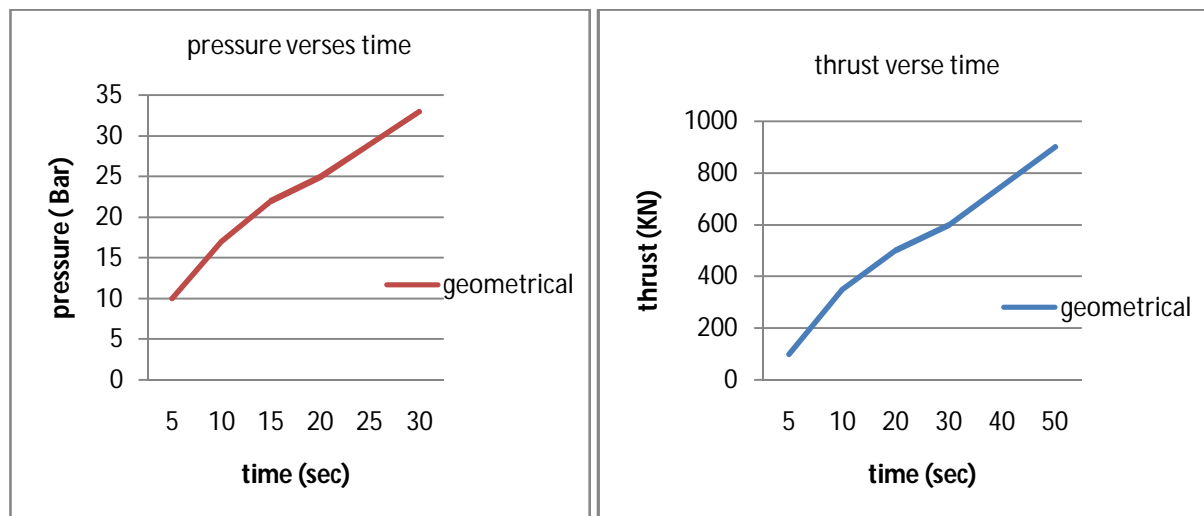


Figure 10: the graphs of pressure/thrust-time

## 5. CONCLUSION

The grain burn back analysis is the one of the most important step of solid rocket motor design. From these work we proposed a simple method of star grain burn back analysis procedure and the attainment of the results from the work. The various results obtained from that work can be compared with some analytical method of grain regression analysis of solid propellant. There are more solid modeling software's, but here we are assumed the CAD, Pro-E and ANSYS design Modular for the development of initial grain geometry with initial parameters. Then the parameters that change during the burnback were adapted for every burn step. The change of the volume of the grain geometry gave the amount of propellant burned for that interval. Dividing this volume by the thickness, the burn area was acquired. Using this data and internal ballistic parameters, the pressure inside the rocket motor was obtained. The method developed in this study not only calculates the burn area, but generates the solid model of the propellant grain for every burn step. These solid models can be used easily for structural analysis without the need for a modification. Also a very important data, the mass properties of the grain geometry, thus the motor altogether, can be achieved from the solid models. These data are very important for flight mechanics at the stage of calculating the final flight path.

## 6. REFERENCES

- [1] S. Fang, K. Hu, P. Zhang and Z. Ma, "A New Simulation Method for 3- D Propellant Grain Burn Analysis of Solid Rocket Motor", AIAA-94-3331, 30th AIANASME/SAE/ ASEE Joint Propulsion Conference, 27-29 June 1994.
- [2] F. Dauch and D. Ribereau, "A Software for SRM Grain Design and Internal Ballistics Evaluation, PffIAL", AIAA-2002-4299, 39<sup>th</sup> AIANASME/ SAE/ ASEE Joint Propulsion Conference & Exhibit, 7-10 July 2002.
- [3] Peterson E G, Nielson C C, Johnson W C, *et al.* Generalized coordinate grain design and internal ballistic evaluation program[R]. AIAA 68-490, 1968.
- [4] Khurram Nisar, Liang Guozhu. Design and optimization of three dimensional finocyl grain for solid rocket motor[R]. AIAA 2008-4696, 2008.
- [5] Khurram Nisar, Liang Guozhu, Qasim Zeeshan. A hybrid optimization approach for SRM finocyl grain design[J]. Chinese Journal of Aeronautics, 2008, 21(6):481-487.
- [6] Dauch F, Ribéreau D. Software for SRM grain design and internal ballistics evaluation, PIBAL[R]. AIAA 2002-4299, 2002.
- [7] A. Ricciardi, "Complete Geometric Analysis of Cylindrical Star Grains", AIAA-1989-2783, 2 5th AIAA/ASME/SAE/ASEE Joint Publication Conference & Exhibit, 10-12 July 1989.
- [8] C. Yildirim and M.H. Aksel, "Numerical Simulation of the Grain Burnback in Solid Propellant Rocket Motor", AIAA-2005- 41 60, 41st AIANASME/SAE/ASEE Joint Propulsion Conference & Exhibit, 10-13 July 2005.
- [9] R.I. Hejl and S.D. Heister, "Solid Rocket Motor Grain Burnback Analysis Using Adaptive Grids", AIAA Journal of Propulsion and Power, Vol 11, No. 5, p 1006-1011, 1995.
- [10] M. A. Willcox, M. Q. Brewster, K.C. Tang and D.S. Stewart, "Solid Propellant Grain Design and Burnback Simulation using a Minimum Distance Function", Journal of Propulsion and Power, Vol. 23, No. 2, p. 465- 475, March-April 2007.
- [11] P.R. Zarda and D.J. Hartman, "Computer-Aided Propulsion Burn Analysis", AIAA-88-3342, 2 4th AIANASME/SAE/ASEE Joint Propulsion Conference, 11-13 July, 1988.



- [12] Grain Design Program, AED Electronics, <http://www.aedelectronics.nl/gdp/gdp.htm>.
- [13] Sutton G.P., Wiley Interscience, Rocket Propulsion Elements, 1992.
- [14] Barrere M. and Jaumotte A. and de Veubeke B. F. and Vandekerckhove J., Elsevier, Rocket Propulsion, 1960.
- [15] Geckler R., Butterworths scientific publications, The mechanism of combustion of solid propellants, 1954.
- [16] J. C. Godon, J. Duterque, and G. Lengellet, JOURNAL OF PROPULSION AND POWER, Vol. 9, No. 6, Erosive Burning in Solid Propellant Motors, 1993.
- [17] H. S. Mukunda and P. J. Paul, COMBUSTION AND FLAME, 109:224-236, Universal Behaviour in Erosive Burning of Solid Propellants, 1997.
- [18] Sethian J.A., Comm. in Math. Phys., 101, 487-499, Curvature and the Evolution of Fronts, 1985.
- [19] Sethian J.A., J. Differential Geometry, 31, 131-161, Numerical Algorithm for propagating Interfaces: Hamilton-Jacobi Equations and Conservation Laws, 1990.
- [20] Sethian J.A., Cambridge Monograph on Applied and Computational Mathematics, Level Set Methods and Fast Marching Methods Evolving Interfaces in Computational Geometry, Fluid Mechanics, Computer Vision, and Materials Science, Cambridge University Press, 1999.
- [20] Plantenga, T.D.: HOPSPACK 2.0 User Manual. SAND2009-6265, Sandia National Laboratories, Albuquerque, USA, 2009.
- [21] Anon.: IMSL: Fortran Subroutines for Mathematical Applications Vol. 2, Visual Numerics, Inc. 1997.
- [22] Johnson, S.G.: The NLOpt nonlinear-optimization package. Available at: <http://ab-initio.mit.edu/nlopt>, 2008, accessed 25 January 2012.
- [23] Digabel, S.L.: Algorithm 909: NOMAD: Nonlinear optimization with the MADS algorithm. ACM Transactions on Mathematical Software, Volume 37, Issue 4, Pages 44-59, 2011.
- [24] Vaz, A.I.F., Vicente, L.N.: PSwarm: A hybrid solver for linearly constrained global derivative-free optimization. Optimization Methods and Software, Volume 24, Issue 4-5, Pages 669-685, 2009.
- [25] Torczon, V.: On the Convergence of Pattern Search Algorithms. SIAM Journal on Optimization, Volume 7, Issue 1, Pages 1-25, 1997.
- [26] Davidson, W.C.: Variable Metric Method for Minimization. SIAM Journal on Optimization, Volume 1, Issue 1, Pages 1-17, 199.
- [27] Abramson, M.A. et al.: OrthoMADS: A deterministic MADS instance with orthogonal directions. SIAM Journal on Optimization, Volume 20, Issue 2, Pages 948-966, 2009.
- [28] Audet, C., Dennis Jr., J.E.: Mesh Adaptive Direct Search Algorithms for Constrained Optimization. SIAM Journal on Optimization, Volume 18, Issue 1, Pages 188-217, 2006.
- [29] Booker, A.J. et al.: A Rigorous Framework for Optimization of Expensive Functions by Surrogates. Structural and Multidisciplinary Optimization, Volume 17, Issue 1, Pages 1-13, 1999.
- [30] Hansen, P., Mladenović, N.: Variable neighborhood search: Principles and applications. European Journal of Operational Research, Volume 130, Issue 3, Pages 449-467, 2001.
- [31] Audet, C., Dennis Jr., J.E., Le Digabel, S.: Parallel Space Decomposition of the Mesh Adaptive Direct Search Algorithm. SIAM Journal on Optimization, Volume 19, Issue 3, Pages 1150-1170, 2008.
- [32] Le Digabel, S. et al.: Parallel Versions of the MADS Algorithm for Black -Box Optimization. Available at [www.gerad.ca/Sebastien.Le.Digabel/talks/2010\\_JOPT\\_25mins.pdf](http://www.gerad.ca/Sebastien.Le.Digabel/talks/2010_JOPT_25mins.pdf), 2010, accessed 31st January 2012.
- [33] Audet, C., Savard, G., Zghal, W. Multiobjective optimization through a series of single objective formulations. SIAM Journal on Optimization, Volume 19, Issue 1, Pages 188-210, 2008.
- [34] Hartfield, R. et al.: A Review of Analytical Methods for Solid Rocket Motor Grain Analysis. AIAA 2003-4506, 39th Joint Propulsion Conference and Exhibit, Huntsville, USA, 2003.